DE GRUYTER OPEN

BUILDING RESEARCH JOURNAL

DOI:10.2478/brj-2014-0008 *VOLUME 61 (2014), NUMBER 2, pp. 101 – 114*

CYCLIC BEHAVIOR OF BRACED CONCRETE FRAMES: EXPERIMENTAL INVESTIGATION AND NUMERICAL SIMULATION

HADAD S. HADAD, IBRAHIM M. METWALLY, SAMEH EL-BETAR

RC shear walls have been widely used as the main lateral-load resisting system in medium and high-rise buildings because of their inherent large lateral stiffness and load resistance. But, in general, the energy dissipating capacity of RC shear walls is not very good and it has been found that using the bracing system gives good results. The main purpose of this paper is to study the effect of different types of bracing on the lateral load capacity of the frame. Also, the research contains a comparison between the braced and infilled frames to decide on the best system. The research scheme consists of four frames; the bare frame, two frames the first of which was braced with concrete, the second was braced with steel bracing and the fourth frame was infilled with solid cement bricks. All the specimens were tested under cyclic loading. The results gave some important conclusions; braced and infilled bare frames increased the lateral strength of the bare frame depending on the type of bracing and infill. Also, the different types of bracing and the infill increased the initial stiffness of the bare frame by a reasonable value. The energy dissipation for the braced and infilled frames is always higher than that for the bare frame up to failure. Also, numerical modeling was carried out with the nonlinear software platform (IDARC). The numerical results obtained with the calibrated nonlinear model are presented and compared with the experimental results. Good agreement was achieved between the numerical simulation and the test results.

Keywords: bracing, infilled frame, cyclic loading; IDARC

1. Introduction

In order to make multi-storey structures stronger and stiffer, i.e. more susceptible to earthquake and wind forces, the cross sections of the member increase from the top to the bottom what makes the structure uneconomical owing to safety of the structure. Therefore, it is necessary to provide a special mechanism and/or mechanisms to improve lateral stability of the structure. Braced frames develop their confrontation to lateral forces by the bracing action of diagonal members. Fully braced frames are more rigid. From saving view point arbitrarily braced ones have least forces induced in the structure and at the same time produce maximum displacement within prescribed limits (Shah and Carve, 2005). In areas of high (sometimes moderate) seismic zones, RC shear walls have been widely used as the main lateral-load resisting system in medium and high-rise buildings because of their inherent large lateral stiffness and load resistance. But, in general, the energy dissipating capacity of RC shear walls is not very good (Xu and Niu, 2003). Until recently, seismic codes used to assign lower behavior for buildings with shear walls than for buildings with frame systems. For instance, in the CEB

Concrete Structures Research Inst., Housing & Building Research Centre, P. O. Box 1770 Cairo, Egypt, e-mail: dr_ibrahimmetwally@yahoo.com

Seismic Code (1985), *q*-factors for frame structures vary from 2.0 to 5.0, for coupled shear walls from 2.0 to 4.0, and for isolated walls from 1.4 to 2.8; it is seen that the values for structures with walls are up to 44 % lower than for frames. In the Uniform Building Code (1994) and Egyptian Code for Loads (2012), the behavior factor (or structural response modification factor) is 50 % lower for buildings with shear walls, compared with ductile frame systems. At the same time shear wall capacity is bigger than frames capacity by more than four to five times so it has been found that one from the most effective and practical methods for enhancing the seismic resistance and increase of the energy absorption capacity of structures is combining two braced elements in the frame. Xu and Niu (2003) found that using the concrete K bracing increases the single frame lateral load capacity by about 250 % and decreases the yield displacement capacity by about 55 %. The value of increase in lateral load capacity was 155 % when using the steel bracing. Youssef et al. (2007) tested three types of steel bracing, and the increases compared with the unbraced one were 215, 150 and 125 % respectively. A 12-story reinforced-concrete building was retrofitted in 1980 after a small earthquake identified seismic deficiencies. Retrofitting included bracing the perimeter frames in the weak (short) direction of the building. The exterior steel truss features heavy steel columns to carry high overturning forces. Truss geometry preserves accessibility to the building and underground parking garage. The slabs were reinforced to transfer shear to new stiff perimeter frames (Aguilar et al., 1996). The aim of this paper is to present the behavior of the steel and concrete cross bracing and its effect on the lateral load capacity and the dissipated energy of the concrete frame and also to compare the braced frame with the infilled frame. Hence, it gives an insight about the strengthening of the concrete frames using crossed steel and concrete frames to increase their lateral load capacity.

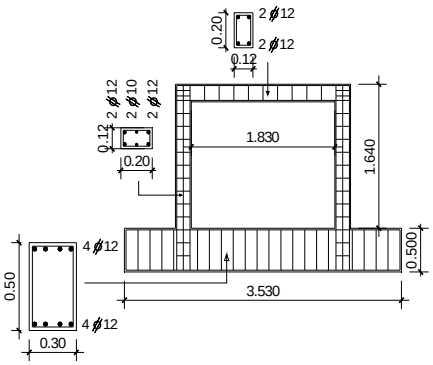

a) Bare Frame Details (F1)

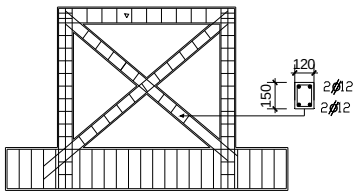

b) Concrete Braced Frame Detail (F2)

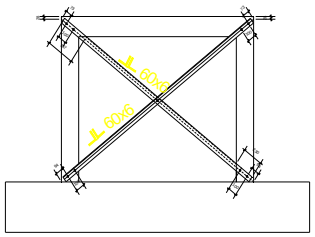

c) Steel Braced Frame Detail (F3)

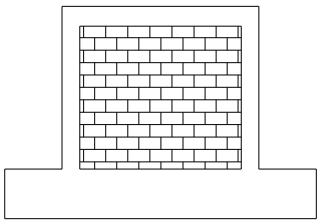

d) Infilled Frame detail (F4)

Figure 1. Specimen reinforcement and details

2. Experimental program

The experimental program consists of four RC frames; specimens F1, F2, F3 and F4. F1 is the bare frame, F2 has a crossed concrete bracing frame, F3 has a crossed steel bracing and F4 has an infill with cement brick. The dimensions and the details of the four specimens are shown in Figure 1. The concrete bracing was cast with the frame and it could be cast after the frame casting and connected to it by sufficient dowels. The steel bracing was connected to the frame using Hilti bolts of 12 mm after the concrete reached its strength (after 28 days).

2.1. Material properties

The concrete mix, used in casting the tested specimens, was developed through trial batches in the Reinforcement Concrete Laboratory of Housing & Building National Research Center (HBRC). The mix was designed to develop concrete cube compressive strength of approximately 27.5 MPa after 28 days. The materials used in the preparation of specimens were ordinary Portland cement, natural sand, well graded crushed head lime stone size No.1 and 2, and tap water respectively. Table 1 shows the quantities required for one cubic meter of fresh concrete to achieve the target concrete cubic compressive strength. High strength deformed steel bars having 12 mm and 10 mm diameters were used. In addition, normal mild smooth steel 6 mm diameter bars were used for stirrups.

Table 1. Proportions of concrete mixes

Constituent	Mix proportion by weight
Cement (kg)	360
Crushed Limestone (kg)	1 200
Sand (kg)	600
Water (liter)	150

Three prisms were taken from the infill of the specimen F4 and tested to evaluate the compression strength of the walls. The compression strength of the prism was 3.8 N/mm^2 and according to the Egyptian code EC-201, (2012) equal to 0.85 of this value.

2.2. Test setup

Figure 2 shows the general arrangement of the test setup and instrumentation system for all tested specimens. The lower beam of the specimen is fixed to the rigid platform by two anchors. A hydraulic jack (J) controlled by a displacement controller is fixed to the steel frame and applies the drift to the concrete specimen through the upper part. The significance of the experimental results from testing schemes might be decided by the accuracy of the measurement of the main output. The main test output in the present setup is the components of the imposed displacement, restoring forces and strains. Displacement transducers were the main devices used for measuring the imposed and resulting displacement in the present test setup. The LVDT's (Linear Voltage Displacement Transducers) used in this particular testing program have an accuracy of

0.10 %, i.e. linear within 0.10 % of the total travel. Their total travel is ± 100 mm. The load cell used is ± 680 MN capacity and output of 5 volt at full scale. The computer controlled load system is available for testing building components. The main components of the testing facility are control station, hydraulic equipment and testing frame. The control station is in conjunction with servo controllers, data acquisition equipment and computer control system. The computer initially receives instructions from the operator and then transmits the signals to the actuator by using the interactive software program. This software has the capability to acquire real-time data through a high speed analog-to digital converter, to control the hydraulic actuator through the servo-controller, and to manipulate.

2.3. Test procedure

During test operation, the specimens were subjected to cyclic loading by a displacement controlled hydraulic jack controlled by a displacement controller. A linear voltage displacement transducer (LVDT'S) was attached to the upper part to measure the lateral deformation. Two linear displacement transducers (main controller) were attached to the two diagonals to measure the diagonal deformation of the specimen. In addition, the strains of the longitudinal steel bars in the test region were measured by two strain gauges attached to the surface of the steel bars for determination of yield limit. The displacement patterns were usually in the form of saw-tooth waves, often with gradually increasing amplitudes. The displacement history was constant for all the tested specimens, the increment of the displacement began with ± 1.0 mm until 10 mm, then the increment increased to be ± 2.0 mm until 20 mm and ± 4.0 mm up to the end of the test.

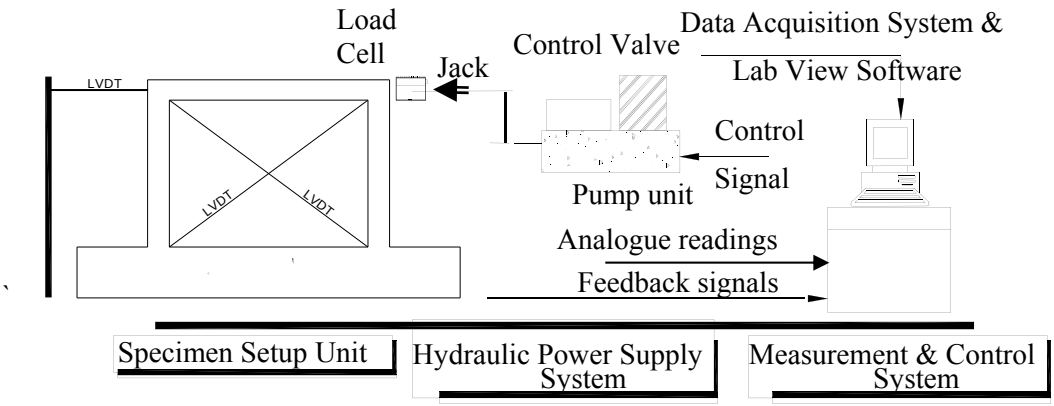

Figure 2. Test Setup

3. Experimental results, analysis and discussion

3.1. Modes of failure

In frame F1 which is considered the bare frame, the cracks began to appear in the column tension side near the column base at about 6 mm top displacement. As the lateral load increased, another cracks appeared near the beam-column connection. At the higher load level diagonal

cracks began to form close and in the beam-column connection. Finally, the failure took place due to the shear failure of the connections as shown in Figure 3.

For concrete braced frame F2, tension cracks started first along the tension side of the diagonal bracings at displacement of 8 to 10 mm. At displacement of 16 to 20 mm cracks started on the compression side of bracing, subsequently, spalling of the concrete cover occurred. After that, buckling of longitudinal bars began. The frame began to deform inelastically. At last plastic hinges took place in the ends of columns and beams as shown in Figure 4.

Frame F3 which had a steel bracing, vertical crack near the base beam at the top and bottom of the inner bolt on the tension side of bracing appeared at 8 – 10 mm displacement. Increasing the lateral top displacement increases the vertical described later crack. Local failure occurred at the column near the lower base beam around the inner bolt on the tension side bracing as shown in Figure 5.

For the infilled frames F4 they approximately had the same behavior and modes of failure as F1. Vertical and horizontal cracks between the frame and the bricks began to appear approximately at the top displacement equal to 4 to 6 mm, then tension cracks in the column near the base and beam column connection appeared at 10 to 14 mm top displacement. With continued cycles, diagonal cracks in the infill formed with separation between the infill and frame. In this case the infill acted as a bracing to the frame. Increased the top displacement level, diagonal cracks in the connection appeared at 15 to 17 mm top displacement. The diagonal cracks of the infill extended, expanded and increased. At the end the infill approximately failed and the specimen began to act as a single frame. Therefore the failure took place due to the shear failure of the beam-column connection for the specimens as shown in Figure 6.

Figure 3. Mode of failure of F1

Figure 4. Mode of failure of F2

Figure 5. Mode of failure of F3

Figure 6. Mode of failure of F4

3.2 Load-Displacement Relationships and Strength Evaluation

The load – displacement hysteresis loops and the strength envelopes of the different specimens are presented in Figures 7 and 8. Also, Table 2 shows the comparison between the load needs for the first cycle (1 mm displacement), the yield displacement, the ultimate load and its equivalent lateral displacement.

As shown from the results, using concrete and steel cross bracing increased the first cycle load from 4.25 KN to 21.6 and 16 KN respectively for framed F2, F3. For the infilled frame F4 the first cycle load was 45 KN which is greater than all the other specimens. Also, the ultimate load for the frame braced with concrete and steel cross bracing were 236.7 and 144 KN which are greater than that of F1 by 200, 142 % respectively and it took place at 26.5 and 21 mm. For F4 the ultimate load was greater than that of the bare frame F1 and F3 by 162 and 8 % respectively but less than that of F2 by 34 %. It is clear that using concrete bracing is more effective than the steel bracing and infilled frame.

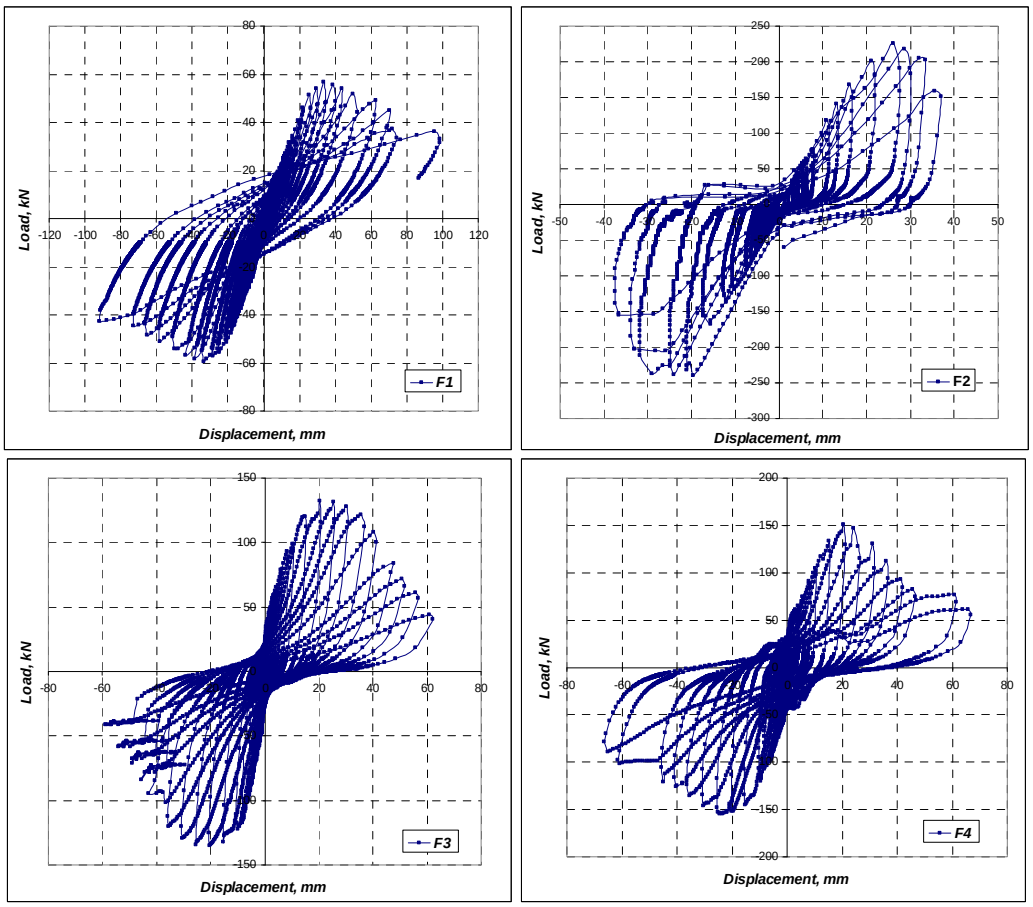

Figure 7. Load-displacement hysteresis curve of specimen F1 (bare frame), F2 (concrete braced frame), F3 (steel braced frame), and F4 (infilled frame)

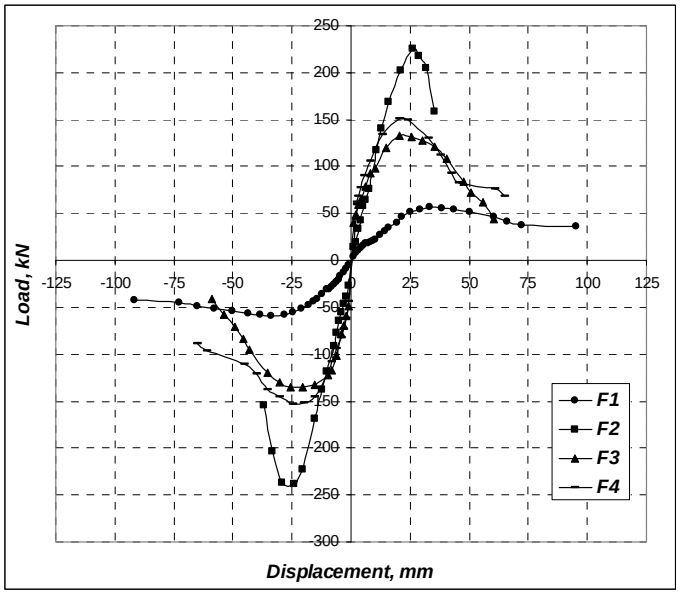

Figure 8. Load-displacement hysteresis envelope of tested specimen

Table 2. Experimental results of tested specimens

Specimen	P_1(first cycle load at 1mm disp), kN	P_u(ultimate load), kN	Δ_u (disp. at P_u), mm	Δ_f (disp. at failure), mm	Δ_y(yield disp.), mm
F1 (bare frame)	4.25	59.3	33.5	59	25
F2 (concrete braced frame)	21.6	236.7	26.5	35	21.5
F3 (steel braced frame)	16	144	21	27.75	18
F4 (infilled frame)	45	155.2	22.08	41	9.0

3.3. Yield, failure displacement, displacement ductility factor and accumulated displacement ductility

The yield displacement for an equivalent elasto-plastic system with reduced cracked stiffness was calculated from the lateral load-displacement curve as the corresponding displacement of intersection of the secant stiffness (at either the first yield or at a load value of 75 % of the ultimate lateral load whichever is less) and a tangent stiffness at the ultimate load. The first yield could not be accurately determined during the test program; hence the evaluation of yield displacement is based on the value of 75 % of ultimate lateral load as shown in Figure 9.

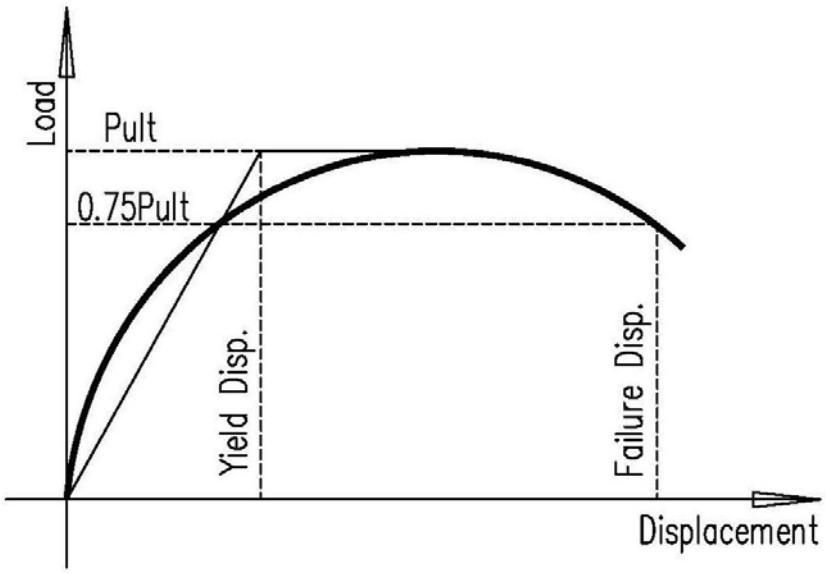

Figure 9. Determination of yield and failure displacement

In cyclically loaded specimens, the strength envelope (Figure 8) was used to determine the yield displacement. Table 2 presents the computed values of yield and failure displacements**.** The previous Figures and the Table 2 show that bracing the bare frame with concrete or steel cross bracing decreased the yield and failure displacement with different values depending on the type of bracing. For the concrete bracing the yield and failure displacement decreased by 14 and 41 % respectively. The steel bracing decreased the yield and failure displacement to18 and 27.75 mm which are smaller than that of the bare frame by 28 and 53 % respectively. If the bare frame infilled using strong bricks as the solid cement bricks the yield and failure displacement decreased by 31 and 64 % respectively. Filling the frame affected the displacement properties of the specimen more than the bracing system.

The displacement ductility is defined as the ratio between the maximum displacement at cyclic number i, Δ_i, and the yield displacement Δ_y.

$$\text{Displacement Ductility} = \Delta_i / \Delta_y \quad (1)$$

Also, the displacement ductility factor is defined as the ratio between the displacement at failure, Δ_f, and the yield displacement Δ_y

$$\text{Displacement Ductility factor} = \Delta_f / \Delta y \quad (2)$$

The accumulated displacement ductility is defined as the sum of the displacement ductility up to the defined failure load as shown in Eq. (3).

$$\text{Accumulated displacement Ductility} = \sum(\Delta_i / \Delta_y) \quad (3)$$

Where Δ_i is the maximum displacement at cycle number i.

Table 3 shows the displacement ductility factors and the accumulated displacement ductility for the test specimens.

Table 3. Displacement Ductility Factor

Specimen	Disp. Ductility Factor	Increasing Ratio, %	Accumulated ductility
F1	2.36	–	20.22
F2	1.63	30.0	9.818
F3	1.54	25.0	7.03
F4	4.5	90.6	21.09

3.4. Energy dissipation characteristics

The capability of a structure to survive an earthquake depends on its ability to dissipate the energy input from ground motion. Despite the fact that energy input during a ground movement event is difficult to estimate, a satisfactory design should ensure a larger energy dissipation capability of the structure than the demand.

The dissipated energy was computed for each cycle as the area enclosed by the lateral load-displacement hysteresis loop for the cycle. The area was computed using Eq. (4).

$$E_i = [(P_i+1+P_i) * (\Delta_{i+1}-\Delta_i)/2] \quad (4)$$

Where:

E_i is the energy dissipated per cycle

P_i and P_{i+1} are the lateral loads at intervals number i, i+1

Δ_i and Δ_{i+1} are the lateral displacement at intervals number i, i+1.

The total accumulated energy of the specimens is shown in Table 4. Also, the plots of the energy dissipation versus lateral displacement of the different specimens are shown in Figure 10. The figure shows that, the infilled frame always has energy dissipation higher than

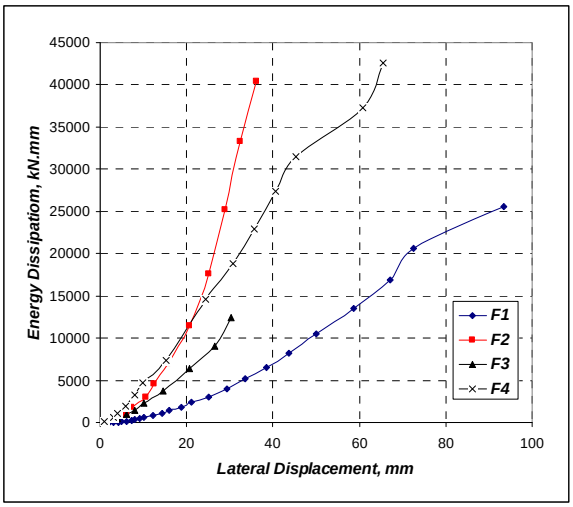

Figure 10. Energy dissipation of the tested specimens

the bare frame up to failure. Infilled frame with cement solid bricks gives the highest energy dissipation capacity. It was about 53, 22, and 153 % higher than that of F1, F2 and F3 respectively. F2 which had concrete bracing gives energy dissipation higher than that of F1, F3 and F4. But F3 which had a steel bracing had the lowest energy dissipation due to that it failed because of the local crashing of concrete around the bolts and the frame itself has some small cracks only.

A non dimensional energy index is used to evaluate the energy dissipated by different test specimens. This energy index is expressed as follows (Ehssani and Wight, 1990):

$$I_{EN} = \sum(E_i\,(K_i / K_y) * (\Delta_i / \Delta_y)^2)/(P_y * \Delta_y) \quad (5)$$

Where:

I_{EN} is the normalized energy index

E_i is the dissipated energy at cycle number i

K_i, K_y are the stiffness at cycle number i and yield respectively

Δ_i, Δ_y are the displacement at cycle i and yield respectively and P_y is the yield load.

The specimen having a normalized energy dissipation index of 60 or higher possesses sufficient ductility to satisfy the intent of ACI-ASCE Committee 352 (2002) recommendations. As shown in Table 4, specimen F4 gives the highest normalized energy index.

Table 4. Comparison between total accumulated energy and the energy index of the specimens

Specimen	Total accumulated energy, kN.mm	I_{EN}
F1	20 570.2	14.3
F2	40 444.6	6.9
F3	12 397.0	3.41
F4	31 428.6	73.23

3.5. Stiffness analysis

The cracked stiffness of each of the specimens was calculated for every loading cycle. The cracked stiffness was computed according to Eq. (6)

$$K_i = P_i / \Delta_i \quad (6)$$

Where:

P_i is the maximum load at cycle i

Δ_i is the maximum displacement at cycle i.

Figure 11 presents the cracked stiffness versus the lateral displacement to represent the stiffness degradation due to cyclic loading. Bracing the frame with any type of bracing or infilling it with a good type of bricks increased the stiffness by reasonable values. The concrete and steel cross bracing increased the stiffness by 3.8, 3.9 times respectively. The concrete and steel bracing increased the stiffness of the bare frame by approximately the same value that may be due to the chosen of the steel bracing section. The infilled frame F4 increased the stiffness by

a great value of 15.34 times the value of F1. After the first cycle the bare frame lost 5 % only from its initial stiffness where it was 12, 17 and 28 % for the specimen F2, F3 and F4 respectively. The stiffness of the bare frame at failure was approximately 15 % from the initial stiffness and it was 29, 18 and 6 % for the specimens F2, F3 and F4 respectively.

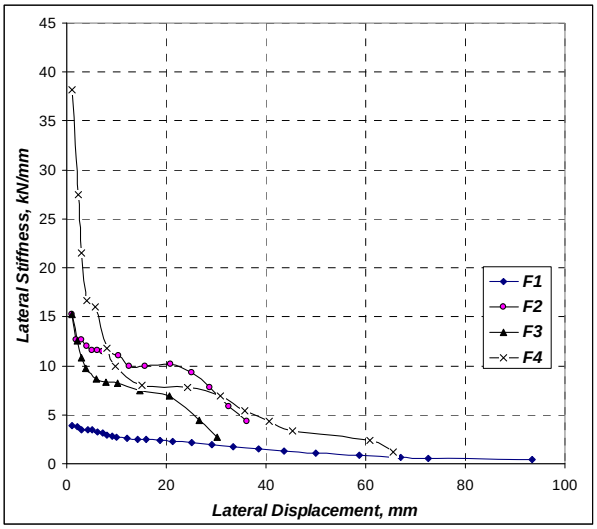

Figure 11. Stiffness degradation of tested specimen

4. Analytical simulation

The load displacement behavior of the test specimens was evaluated by using the nonlinear analysis software namely IDARC-2D (Reinhorm et al., 2004). The computer program IDARC (ver. 6) is used to simulate the observed experimental results. Column elements were modeled considering macromodels with inelastic flexural deformations, and elastic shear and axial deformations. Beam elements are modeled using a nonlinear flexural stiffness model with linear elastic shear deformations considered. Shear walls include inelastic shear and bending deformations, with an uncoupled elastic axial component. In addition to force and deformations the computer program calculates the damage index for each member as well as for all frames which represents the frame state under cyclic loading.

The studied frames were analyzed by the program under in plane quasi-static cyclic loading controlled by displacement. Figure 12 shows the comparison between experimental results and analytical ones by IDARC for control frame (F1), shear wall (concrete braced frame (F2)) and infilled frame (F4). Good agreement was noticed between test results and analytical ones as shown in Figure 12 and also in Table 5. The average experimental/predicted values of ultimate load capacity and failure displacement are very close to one (1.02 and 1.05 respectively), this indicates the accuracy of IDARC upon nonlinear cyclic analysis of RC frames.

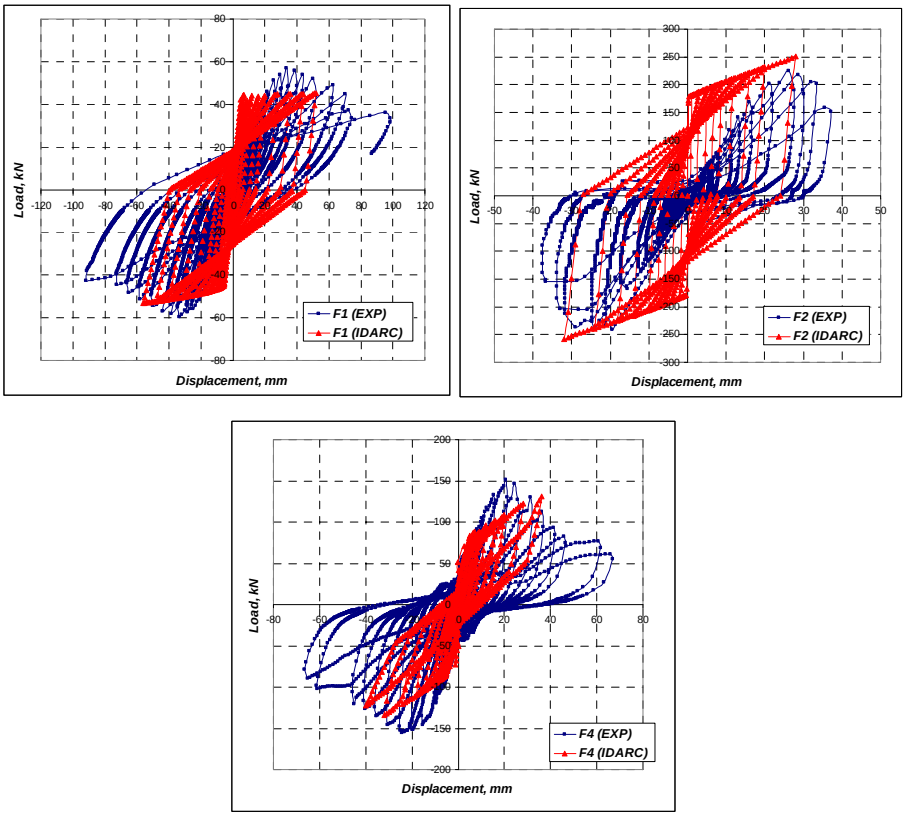

Figure 12. Comparison of experimental versus simulated load-displacement response of test frame specimen: bare frame (F1), concrete braced frame (F2) and infilled frame (F4)

Table 5. Comparison between experimental results and ones predicted by IDARC

Specimen	Experimental results		Results predicted by IDARC		Exp/Pred	
	P_u (ultimate load), kN	Δ_f (disp at failure), mm	P_u (ultimate load), kN	Δ_f (disp at failure), mm	P_u	Δ_f
F1 (bare frame)	59.3	59	53.11	56	1.11	1.05
F2 (concrete braced frame)	236.7	35	257.5	32	0.92	1.09
F4 (infilled frame)	155.2	41	149	40	1.04	1.02
Mean					1.02	1.05
Standard deviation					0.096	0.03

5. Damage analysis

Important research efforts have been carried out to develop an accurate damage index to qualify the response of structures. The response index is used to estimate the damage in RC members as developed by Park and Ang (1985).

The damage model accounts for damage due to maximum inelastic excursions, as well as damage due to the history of deformations. Damage index for a structural element is defined as:

$$DI = \frac{\theta_m - \theta r}{\theta_u - \theta_r} + \frac{\beta}{M_y \theta_u} E_h \tag{7}$$

Where:

θ_m is the maximum rotation attained during the loading history

θ_u is the ultimate rotation capacity of the section

θ_r is the recoverable rotation when unloading

M_y is the yield moment

E_y is the dissipated energy in the section.

The element damage is then selected as the biggest damage index of the end sections.

To demonstrate the effect of infill on the behavior of existing structures under lateral loads, a global value of damage index can be used to characterize damage in the RC frames. The overall structural damage (OSD) of F1 and F4 are 0.13 and 0.092 respectively. F4 recorded the lower value of OSD compared to bar frame, this refers to the infill reduces the large deformation that causes the damage. It is concluded that removing the walls in the RC old buildings should be limited especially for weak skeleton structures.

6. Conclusions and recommendations

1. Using any type of bracing increases the lateral strength of the bare frame depending on the type of bracing. The increase of lateral strength of concrete and steel bracing was 200, 142 % respectively.
2. Cracks in infill material and separation from the surrounding concrete frames took place at early stages of failure and that was clear in specimen F4.
3. The energy dissipation for the braced and infilled frames is always higher than that for the bare frame up to the failure. The increased values were 20, 18 and 21 % that of the bare frame for frames F2, F3 and F4 respectively.
4. The different types of bracing increased the initial stiffness of the bare frame by reasonable values. The concrete and steel bracing increased the stiffness of the bare frame by 280, 290 % respectively.
5. It is preferred to infill some regions in the building frames with reasonable strength bricks to improve the lateral stiffness of these buildings. Using the infill from solid cement bricks increased the stiffness of the bare frame 15.34 times.
6. The force-displacement response of bare and braced frames was reproduced well using the nonlinear program, IDARC. Reasonably good agreement between experimental measurements and analytical results has been observed for the global behavior of the braced frames.

7. The solid brick walls infill has a significant effect to resist earthquakes which reduces the large deformation that causes the damage. So, removing the walls in the RC old buildings should be limited especially for weak skeleton structures.
8. However, further research work is needed in order to achieve more economy by developing new types of bracing. This work is important, because braced frames are a very efficient and effective system for resisting lateral forces. Also, it is very needed to show experimentally the effect of bracing upon multi bay and storey frames.

References

[1] ACI-ASCE Committee 352 (2002), Recommendations for Design of Beam-Column Connections in Monolithic Reinforced Concrete Structures, American Concrete Institute.

[2] Aguilar, J., Brena, S. F., Del Valle, E., Iglesias, J., Picado, M., Jara, M. and Jirsa, J. O. (1996), Rehabilitation of Existing Reinforced Concrete Buildings in Mexico City. PMFSEL-96-3, The University of Texas at Austin.

[3] Committee Euro-International du Beton (CEB) (1985), Model Code for Seismic Design of Concrete.

[4] Egyptian Code for Loads Calculations in the Structural and Building Works (EC-201) (2102), Housing & Building National Research Centre.

[5] Ehssani, M. R. and Wight, J. K. (1990), Confinement Steel Requirements for Connection Ductile Frames. Journal of Structural Engineering, 116, 450-465.

[6] Park, Y. J. and Ang, A. H. S. (1985), Mechanistic seismic damage in reinforced concrete. Journal of Structural Eng., 111, 722-739.

[7] Reinhorm, A. M., Kunnath, S. K. and Valles, R. E. (2004), IDARC2D, A Computer Program for Inelastic Damage Analysis of Buildings. Version 6, Department of Civil Engineering, State University of New York at Buffalo.

[8] Shah, V. and Karve, S. (2005), Illustrated Design of Reinforced Concrete Buildings, 5th Ed., Structures Publication, Parvati.

[9] Uniform Building Code (UBC) (1994), International Conference of Building Officials (ICBO).

[10] Xu, S. and Niu, D. (2003), Seismic Behavior of Reinforced Concrete Braced Frame. ACI Structural Journal, 100, 120-125.

[11] Youssef, M., Ghaffarzadeh, H. and Nehdi, M. (2007), Seismic Performance of RC Frames with Concentric Internal Steel Bracing. Engineering Structures, 29, 1561-1568.